

Effect of Embossed Straight Plastic Fibres with Varying Aspect Ratios on Compressive and Flexural Behaviour of OPC 53 Grade Cement Based Geopolymer ConcreteAditya L¹, Meena Y R²¹Research Scholar, Department of Civil Engineering, JAIN (Deemed-to-be University), Bengaluru- 562112, Karnataka, India²Associate Professor and PG Program Head, Department of Civil Engineering, JAIN (Deemed-to-be University), Bengaluru- 562112, Karnataka, India
Corresponding author's email: adityalak1995@gmail.com**Abstract**

Conventional OPC-based concrete is a major contributor to global CO₂ emissions, driving the need for sustainable binder alternatives such as geopolymer concrete that utilise industrial by-products like fly ash. However, geopolymer concrete inherently exhibits brittle failure behaviour, and the role of embossed straight polypropylene fibres, particularly the effect of varying aspect ratios on its mechanical performance remains insufficiently studied under Indian Standards. This experiment examines the influence of embossed straight plastic fibres (diameter 0.6 mm, lengths 30, 45, 60, 75 mm) added at 0%, 0.5%, 1.0%, 1.5% and 2.0% by volume to a hybrid geopolymer concrete using OPC 53 grade cement (IS 12269) blended with Class F fly ash. The binder comprised 70% Class F fly ash and 30% OPC 53, with a total binder content of 420 kg/m³. A 12 M sodium hydroxide solution and sodium silicate solution (Na₂SiO₃/NaOH = 2.5 by mass) were used as the alkaline activator system, with an activator-to-binder ratio of 0.40. Compressive strength (100 mm cubes) and flexural behaviour (100×100×500 mm prisms, two-point loading per IS 516) were evaluated at 28 days. Workability was assessed by slump test per IS 1199 (Part 2):2018. Results indicate 1.5% fibre volume gives the best balance of retained compressive strength and substantially improved flexural toughness and residual load capacity, with flexural toughness increasing up to 10 times compared to the control.

Keywords — Geopolymer concrete; polypropylene fibres; flexural toughness; compressive strength; fly ash; alkaline activator; aspect ratio**1. INTRODUCTION**

The global construction sector accounts for approximately 8% of worldwide CO₂ emissions, with Portland cement production alone responsible for 5–8% of anthropogenic greenhouse gas output [12, 35]. In India, rapid urbanisation and large-scale infrastructure expansion have made this environmental burden particularly acute: the country is among the world's top three cement producers, and demand is projected to grow at 6–7% annually through 2030 [23, 36]. This reality creates a compelling imperative to develop low-carbon alternatives to Ordinary Portland Cement (OPC) that can meet the structural performance requirements of Indian Standards without sacrificing durability or cost-effectiveness.

Geopolymer binders, first systematically described by Davidovits [12], offer a compelling solution. By activating aluminosilicate precursors such as Class F fly ash with alkaline solutions of NaOH and Na₂SiO₃, it is possible to produce a cementitious binder whose embodied CO₂ footprint is 40–80% lower than that of OPC [22, 35]. Fly ash, a by-product of coal-fired thermal power stations, is generated in enormous quantities in India – exceeding 200 million tonnes per year – yet remains significantly underutilised [36]. Replacing the bulk of OPC with fly ash in a geopolymer binder simultaneously reduces carbon emissions and converts an industrial waste stream into a structural material, directly aligning with both the Bureau of Indian Standards' push for sustainable construction materials and India's Nationally Determined Contributions under the Paris Agreement. However, a well-established limitation of geopolymer and fly ash-based concrete systems is their inherently brittle post-crack behaviour [14, 22]. Plain geopolymer concrete, much like plain OPC concrete, exhibits a near-instantaneous loss of load-carrying capacity once the tensile stress at the extreme fibre exceeds the matrix tensile strength. This brittleness is particularly problematic in structural applications such as slabs, beams, and pavement that are subjected to flexure, impact, or cyclic loading – scenarios where post-crack ductility and energy absorption are critical safety requirements [15, 30]. Addressing this limitation through fibre reinforcement is therefore not merely a performance enhancement but a structural necessity for geopolymer concrete to be accepted as a viable alternative in mainstream Indian construction practice.

Fibre reinforcement has long been recognised as an effective strategy to transform brittle cementitious matrices into pseudo-ductile composites [15, 19, 31]. Among the many fibre types available – steel, glass, basalt, carbon, and synthetic – polypropylene (PP) fibres present a uniquely attractive combination of properties for the Indian context: they are chemically inert and corrosion-resistant in highly alkaline environments such as geopolymer matrices [28], they are substantially lighter than steel (density ≈ 0.92 g/cm³ versus 7.8 g/cm³), they are considerably less expensive, and they are readily available domestically [16, 20]. The addition of PP fibres at low volume fractions (0.5–2.0%) has been shown to dramatically improve flexural toughness, crack-width control, and post-crack load retention in OPC concrete, while having only a marginal effect on compressive strength [16, 20, 29]. Despite this promise, the body of literature on PP fibre-reinforced geopolymer concrete remains limited compared to that for OPC systems, and key questions remain unanswered. In particular, the influence of fibre aspect ratio (length-to-diameter ratio) on the mechanical response of hybrid geopolymer – OPC systems has received little systematic attention [28, 37]. Fibre geometry profoundly affects both fresh-state behaviour (workability, fibre dispersion) and hardened-state performance (crack-bridging efficiency, pull-out resistance, and interfacial bond development) [15, 26, 27]. The embossed surface texture on straight PP fibres, which increases mechanical interlock with the matrix, adds a further variable that has not been isolated and quantified in geopolymer systems under Indian Standards testing protocols. There is therefore a clear knowledge gap: the combined effect of fibre length, volume fraction, and surface texture on both compressive and flexural performance of hybrid geopolymer concrete tested to IS 516 has not been comprehensively established. The hybrid approach adopted in this study – replacing 70% of the binder with Class F fly ash while retaining 30% OPC 53 grade cement – is motivated by practical considerations as much as environmental ones. Pure fly ash geopolymers require elevated-temperature curing or extended ambient curing periods to develop adequate early strength, which limits their field applicability [13, 33, 34]. The inclusion of OPC introduces calcium silicate hydrate (C–S–H) gel alongside the N–A–S–H geopolymer gel, accelerating setting and permitting oven curing at the modest temperature of 60 °C for 24 hours – a regime feasible in precast production [34]. The alkaline activator system comprising 12 M NaOH and Na₂SiO₃/NaOH ratio of 2.5 is consistent with the optimum values established by Hardjito and Rangan [13] and corroborated by Patankar et al. [32], and the activator-to-binder ratio of 0.40 falls within the published optimum range of 0.40–0.50 for fly ash–OPC hybrid systems [32]. All testing follows Indian Standards (IS 516, IS 1199) to ensure the results are directly applicable to Indian design and construction practice. Against this background, the present study was undertaken to systematically investigate the effect of embossed straight polypropylene fibres of four lengths (30, 45, 60, and 75 mm; diameter 0.6 mm; aspect ratios 50, 75, 100, and 125 respectively) at five volume fractions (0%, 0.5%, 1.0%, 1.5%, and 2.0%) on the compressive and flexural behaviour of a hybrid geopolymer concrete with a 70:30 fly ash:OPC 53 binder. The central motivation is two-fold: first, to demonstrate that geopolymer concrete can achieve structural-grade compressive strength (40–45 MPa) while radically improving post-crack ductility through appropriately chosen PP fibre reinforcement; and second, to identify the optimal fibre length and dosage combination so that practitioners, precast manufacturers, and code committees in India have an evidence base for incorporating fibre-reinforced geopolymer concrete in IS 456-governed structural design. By generating data against IS 516 test protocols, this work directly bridges the gap between international geopolymer research and Indian engineering practice.

OBJECTIVES

- Quantify 28-day compressive strength variation with fibre length and volume fraction.
- Measure flexural behaviour (first-crack load, peak load, residual loads, toughness indices) per IS procedures.
- Identify optimum fibre volume fraction and length for best flexural toughness with acceptable compressive strength.
- Compare findings qualitatively with literature on plastic fibres in OPC and geopolymer concrete.
- Provide practical recommendations for mix design and field implementation using IS procedures.

2. STANDARDS AND CODES (INDIAN STANDARDS)

- IS 12269 : 2013 — Specification for 53 grade Ordinary Portland Cement.
- IS 3812 (Part 1) : 2003 — Pulverized fuel ash for use as pozzolana.
- IS 3883 : 2016 — Specification for coarse and fine aggregates for concrete.
- IS 2386 (Parts 1–8) — Methods of test for aggregates for concrete.
- IS 10262 : 2019 — Concrete mix proportioning — Guidelines.
- IS 1199 (Part 1) : 2018 — Sampling of fresh concrete [6]. IS 1199 (Part 2) : 2018 — Slump test for workability of fresh concrete [7].
- IS 516 (Part 1, Sec 1) : 2018 — Compressive strength of concrete [8]. IS 516 (Part 5, Sec 1) : 2018 — Flexural strength of concrete [9].
- IS 456 : 2000 — Code of practice for plain and reinforced concrete.
- IS 9103 : 1999 — Specification for admixtures for concrete.

3. MATERIALS

Binder: OPC 53 grade cement conforming to IS 12269 [1]. Class F fly ash conforming to IS 3812 (Part 1) [2]. Binder proportion: fly ash : OPC = 70 : 30 (hybrid geopolymer approach). Total binder content: 420 kg/m³. Fly ash content: 294 kg/m³; OPC content: 126 kg/m³.

Alkaline Activator: Sodium hydroxide (NaOH) solution prepared at 12 M concentration — NaOH pellets dissolved in distilled water (approximately 404 g NaOH solids per kg of solution) and allowed to cool for 24 hours before use. Sodium silicate (Na₂SiO₃) solution mixed with NaOH solution at a mass ratio of 2.5, consistent with the optimum ratio reported in [13]. NaOH solution: 48 kg/m³; Na₂SiO₃ solution: 120 kg/m³; Total activator: 168 kg/m³; Activator-to-binder ratio: 0.40.

Aggregates: Fine aggregate: M-Sand, Zone II per IS 383 [3]: 700 kg/m³. Coarse aggregate: crushed granite 10–20 mm per IS 383: 1100 kg/m³. Aggregate tests conducted per IS 2386 [4].

Fibres: Embossed straight polypropylene (PP) fibres, diameter 0.6 mm, lengths 30 mm, 45 mm, 60 mm and 75 mm. Density = 0.92 g/cm³. Supplied in cut form; embossed surface improves mechanical interlock with the matrix.

Admixture: Polycarboxylate ether-based superplasticizer conforming to IS 9103 [11] to maintain workability. Dosage adjusted with increasing fibre content (see Section 7.1 and Appendix A). Additional water: 30 kg/m³, added to assist workability and OPC hydration. Total mix density ≈ 2418 kg/m³.

4. MIX DESIGN AND SPECIMEN MATRIX

Mixes: 4 fibre lengths × 5 fibre volume fractions = 20 mixes; 3 trial specimens per mix; total specimens = 60. Fibre contents: 0.0%, 0.5%, 1.0%, 1.5%, 2.0% by volume. Control mix: 0% fibres (all four fibre-length series share the same 0% control proportions). Mix proportioning followed IS 10262:2019 [5] guidelines adapted for geopolymer concrete [33].

Specimens: Compressive: 100 mm cubes, 3 specimens per mix, tested per IS 516 (Part 1, Sec 1):2018 [8]. Flexural: 100×100×500 mm prisms, 3 specimens per mix, two-point loading per IS 516 (Part 5, Sec 1):2018 [9]. Curing: initial ambient curing 24 hours; oven curing at 60 °C for 24 hours (geopolymer activation); then ambient curing to 28 days.

5. EXPERIMENTAL PROCEDURE

Activator Preparation: Prepare 12 M NaOH solution (≈404 g NaOH pellets per kg solution); allow to cool for 24 hours. Combine NaOH solution (48 kg/m³) and Na₂SiO₃ solution (120 kg/m³) at a mass ratio of 2.5 : 1 (Na₂SiO₃ : NaOH). Allow combined activator to equilibrate for at least 30 minutes before use.

Mixing Sequence

- (1) Dry mix binder (fly ash + OPC) and aggregates for 2 minutes.
- (2) Add fibres gradually during dry mixing to avoid balling; continue for 1 minute.
- (3) Add combined alkaline activator and 50% of superplasticizer; mix for 3–4 minutes until uniform.
- (4) Adjust superplasticizer dosage to achieve target slump per IS 1199 (Part 2):2018 [7]; the effect of superplasticizer type on geopolymer workability is documented in [21].

Testing

Workability: slump test per IS 1199 (Part 2):2018 [7]; three measurements per mix. Compressive test: IS 516 (Part 1, Sec 1):2018 [8]; loading rate 140 kg/cm²/min; record peak load and compute compressive strength. Flexural test: two-point loading per IS 516 (Part 5, Sec 1):2018 [9]; span = 400 mm; mid-span deflection measured with dial gauge/LVDT; record load–deflection curve at 0.5 mm intervals; determine first-crack load, peak load, residual loads at 1 mm and 3 mm deflections, and compute flexural toughness (area under curve to 3 mm) following ASTM C1609 [18] principles. Test minimum 3 specimens per data point; report mean and standard deviation.

APPENDIX A — MIX PROPORTIONS FOR ALL MIXES (PER M³)

Binder content revised to 420 kg/m³ (OPC 53: 126 kg; Fly Ash: 294 kg). Activator: NaOH 12 M = 48 kg, Na₂SiO₃ = 120 kg, Total = 168 kg, A/B ratio = 0.40. Extra water = 30 kg/m³. Fibre density = 0.92 g/cm³ (PP). Total mix density ≈ 2418 kg/m³. Adjust per IS 10262:2019 [5] and laboratory trial mixes. Fly Ash = 294 kg, OPC 53 = 126 kg, Fine Agg. = 700 kg/m³, Coarse Agg. = 1100 kg/m³, NaOH 12M = 48 kg/m³, Na₂SiO₃ = 120 kg/m³ Water = kg/m³

Table A1 - Mix proportions for all mixes (per m³)

Length (mm)	Fibre (% vol)	OPC 53 (kg)	Fly Ash (kg)	SP (% bdr)	Fibre (kg)
30	0.0	126	294	1.0	0.00
30	0.5	126	294	1.0	0.46
30	1.0	126	294	1.3	0.92
30	1.5	126	294	1.6	1.38
30	2.0	126	294	1.9	1.84
45	0.0	126	294	1.0	0.00
45	0.5	126	294	1.0	0.69
45	1.0	126	294	1.3	1.38
45	1.5	126	294	1.6	2.07
45	2.0	126	294	1.9	2.76
60	0.0	126	294	1.0	0.00
60	0.5	126	294	1.0	0.92
60	1.0	126	294	1.3	1.84
60	1.5	126	294	1.6	2.76
60	2.0	126	294	1.9	3.68
75	0.0	126	294	1.0	0.00
75	0.5	126	294	1.0	1.15
75	1.0	126	294	1.3	2.30
75	1.5	126	294	1.6	3.45
75	2.0	126	294	1.9	4.60

Notes: (1) NaOH at 12 M (≈404 g/kg solution); prepare 24 h before use. (2) Na₂SiO₃/NaOH mass ratio = 2.5 per [13]. (3) Total activator = 168 kg/m³; A/B ratio = 0.40. (4) SP varies with fibre volume fraction; adjust in laboratory trials. (5) Fibre density = 0.92 g/cm³ (PP).

6. DATA PROCESSING AND INDICES

Compressive Strength

Compressive strength is computed as: $f_c = P_{max} / A$, where P_{max} is the peak load and A is the cross-sectional area of the specimen (mm²).

Flexural Toughness

Toughness (kN·mm) = area under the load–deflection curve up to 3 mm deflection, computed by trapezoidal rule: $T = \sum [(F_i + F_{i+1}) / 2 \times \Delta\delta]$, where F is load (kN) and δ is deflection (mm). Residual strength indices: residual load at 1 mm and 3 mm deflection normalised by the first-crack load.

7. RESULTS

7.1 Workability — Slump Test Results

Slump was measured per IS 1199 (Part 2):2018 [7]. Table 1 presents mean results from three measurements per fibre content level; all fibre lengths showed comparable workability trends for the same volume fraction.

Table 1 Slump and superplasticizer demand by fibre volume fraction

Fibre Volume (%)	Slump (mm)	SP Dosage (% by binder mass)	Observations
0.0	120	1.0	Workable; no fibre balling; suitable for all placement methods
0.5	100	1.0	Minor workability reduction; admixture at base dosage; good workability
1.0	75	1.3	Moderate reduction; admixture +0.3% by binder mass; acceptable workability
1.5	55	1.6	Stiff but workable; admixture +0.6%; careful placing and compaction needed
2.0	30	1.9	Noticeable fibre balling; admixture +0.9%; marginal workability; not recommended

As seen in Table 1, slump decreased progressively from 120 mm at 0% fibres to 30 mm at 2.0% volume fraction, with a corresponding rise in superplasticizer (SP) demand from 1.0% to 1.9% by binder mass. The reduction is attributable to the high surface area of PP fibres absorbing the free water film in the paste, increasing internal friction and restricting flow. At 0.5% and 1.0% fibre volume, workability remained in the medium range (IS 456 [10]) and SP dosage could be maintained near the base level, indicating good practical compatibility. At 1.5%, the slump of 55 mm is still adequate for vibrated placement provided SP is adjusted to 1.6% by binder mass. Beyond 1.5%, however, the onset of fibre balling caused a sharp non-linear drop to 30 mm at 2.0%, making uniform compaction in field conditions unreliable. This workability boundary at 1.5% is one of the key factors that corroborates it as the practical optimum dosage.

7.2 Compressive Strength (28 days) — 100 mm Cubes

The 28-day compressive strength results for all mixes are presented in Figure 1. A small strength gain is observed up to 1.0–1.5% fibre volume, attributable to crack-arresting and matrix confinement effects. A slight reduction at 2.0% is associated with increased entrapped air and compaction difficulties at higher fibre dosages.

Figure 4 — 28-day Compressive Strength vs. Fibre Volume Fraction (All Fibre Lengths, 100 mm Cubes, IS 516)

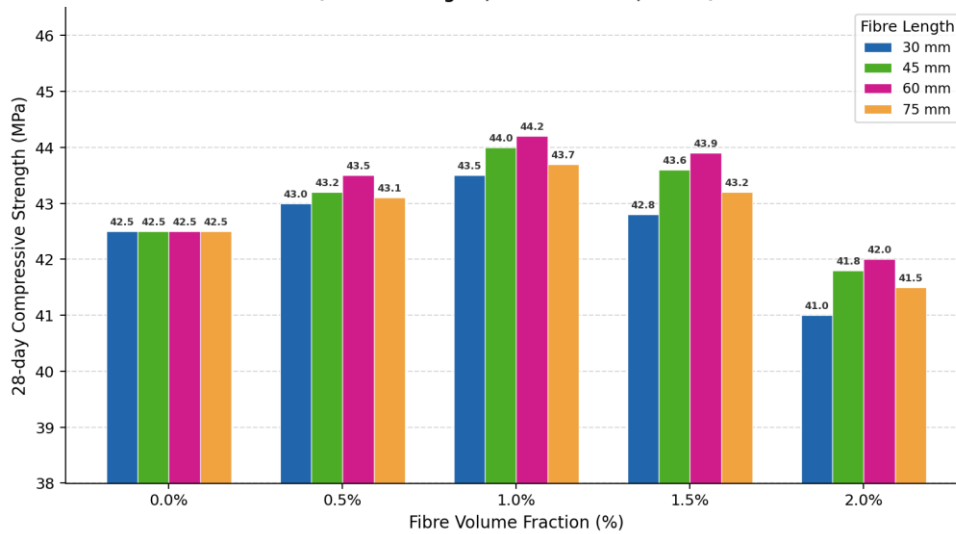


Figure 1 — 28-day Compressive Strength vs. Fibre Volume Fraction (All Fibre Lengths, 100 mm Cubes, IS 516)

The compressive strength data are presented in Figure 1, which plots 28-day strength against fibre volume fraction for all four fibre lengths. All length series follow a consistent inverted-U profile: strength rises marginally from the control value of 42.5 MPa to a peak at 1.0% (43.5–44.2 MPa depending on length), then falls slightly at 1.5% before declining more noticeably at 2.0%. The 60 mm fibre series consistently achieved the highest values across all dosages, reaching 44.2 MPa at 1.0% — a gain of 1.7 MPa (4.0%) over the control. The improvement at low dosages reflects micro-crack bridging and passive confinement of the matrix by the fibres. The decline at 2.0% (down to 41.0–42.0 MPa across lengths) is consistent with increased void content from incomplete compaction when fibre balling occurs. Crucially, the maximum deviation from the control at any dosage is within ±5%, confirming that the addition of PP fibres does not compromise the structural compressive performance of the hybrid geopolymer matrix.

7.3 Flexural Results — 100×100×500 mm Prisms (Two-Point Loading)

The key flexural parameters for all mixes are presented graphically in Figures 2 and 3 (below). Flexural toughness and residual load capacity increase markedly up to 1.5% fibre volume, particularly for 60 mm fibres. A marginal decline is observed at 2.0% attributable to workability reduction and fibre clustering. The control mix exhibits brittle failure with negligible post-crack residual capacity.

Figure 2 — Flexural Toughness vs. Fibre Volume Fraction (All Fibre Lengths, 100×100×500 mm Prisms, IS 516)

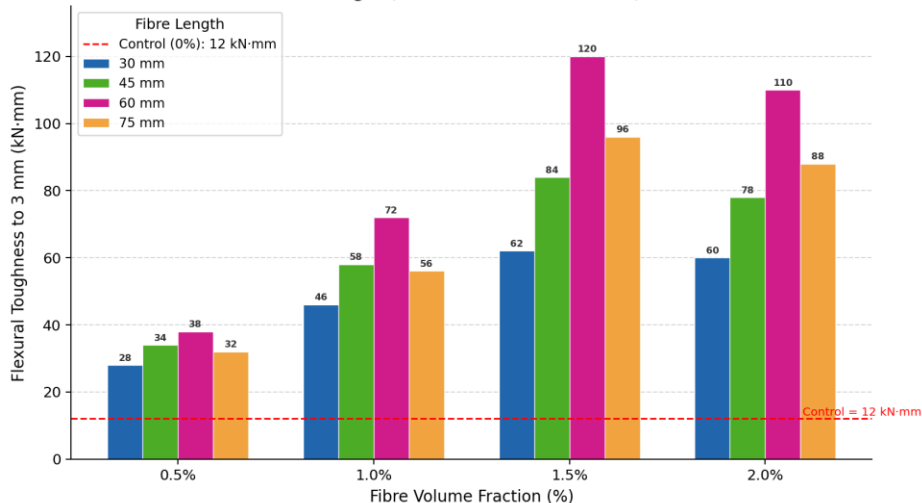


Figure 2 — Flexural Toughness to 3 mm vs. Fibre Volume Fraction (All Fibre Lengths, IS 516)

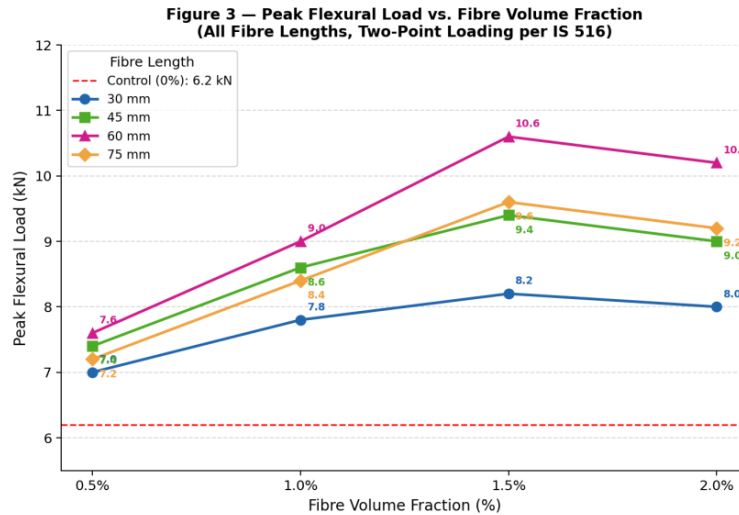


Figure 3 — Peak Flexural Load vs. Fibre Volume Fraction (All Fibre Lengths, IS 516)

Figure 2 presents flexural toughness ($\text{kN}\cdot\text{mm}$) as a grouped bar chart for all fibre lengths and volume fractions, making the dominant influence of both fibre length and dosage immediately apparent. Toughness rose sharply with increasing volume fraction for all lengths, reaching a clear peak at 1.5% before declining marginally at 2.0%. The 60 mm fibre series achieved the highest toughness at every dosage level, culminating in $120 \text{ kN}\cdot\text{mm}$ at 1.5% — a ten-fold improvement over the control value of $12 \text{ kN}\cdot\text{mm}$. The 75 mm series reached $96 \text{ kN}\cdot\text{mm}$ at 1.5%, and although this represents a substantial gain, it falls short of the 60 mm series owing to the greater practical difficulty of dispersing longer fibres uniformly. The 30 mm series showed the lowest toughness gains ($62 \text{ kN}\cdot\text{mm}$ at 1.5%), reflecting the limited crack-bridging capacity of shorter fibres whose embedment length may be insufficient to develop full bond across wide macro-cracks. The consistent decline from 1.5% to 2.0% across all length series in Figure 2 confirms that the workability and compaction penalties of higher fibre dosages directly translate into reduced energy absorption capacity. Figure 3 plots peak flexural load against fibre volume fraction for all lengths. The curves exhibit a monotonically increasing trend up to 1.5%, followed by a slight drop at 2.0%. The 60 mm series again leads, with peak load increasing from 6.2 kN (control) to 10.6 kN at 1.5% — a 71% improvement. The 45 mm and 75 mm series reached 9.4 kN and 9.6 kN respectively at 1.5%, while 30 mm fibres achieved 8.2 kN. The spread between length series narrows at low dosages (0.5%) and widens progressively at higher dosages, indicating that fibre length has a greater influence on peak load as the fibre network becomes denser. Taken together, Figures 2 and 3 establish 60 mm fibres at 1.5% by volume as the optimal combination for maximising both peak load-carrying capacity and post-crack energy absorption.

7.4 Load-Deflection Behaviour

Control specimens failed in a brittle manner at first crack, with negligible post-crack capacity and total energy absorption limited to $12 \text{ kN}\cdot\text{mm}$. At 1.5% (60 mm fibres), a ductile response was observed with a significant post-crack plateau and multiple load-drops-and-recoveries due to fibre bridging; the peak load (10.6 kN) was reached at approximately 1.5–2.0 mm deflection, sustaining residual capacity to 3 mm and beyond (energy absorption = $120 \text{ kN}\cdot\text{mm}$; 10-fold increase over control). At 2.0% (60 mm fibres), toughness was marginally lower ($110 \text{ kN}\cdot\text{mm}$), confirming 1.5% as the practical optimum.

Refer to Figure 4 (load-deflection curves), Figure 2 (toughness bar chart), Figure 3 (peak load line chart) and Figure 1 (compressive strength bar chart) for graphical representations of these results. Figure 4 presents the load-deflection curves for the 60 mm fibre series at all five volume fractions under two-point loading per IS 516. The response of the control specimen (0% fibres) is characterised by a linear elastic rise to first-crack load (6.2 kN at approximately 0.25 mm deflection), followed immediately by a sudden brittle failure with load dropping to near zero, yielding a toughness of just $12 \text{ kN}\cdot\text{mm}$. This is the classic plain-concrete response, and it establishes the baseline against which fibre contributions are measured. With the introduction of 0.5% fibre volume, the post-crack region transforms markedly: a residual load of 1.2 kN is sustained at 3 mm deflection, and toughness rises to $38 \text{ kN}\cdot\text{mm}$ — a three-fold increase over the control. As volume fraction increases to 1.0%, the peak load rises to 9.0 kN and the post-crack plateau broadens, with energy absorption reaching $72 \text{ kN}\cdot\text{mm}$. The 1.5% curve demonstrates the most favourable shape: a gradual post-peak softening with multiple load-recovery events (characteristic of sequential fibre pull-out and bridging across macro-cracks), sustaining a residual load of 3.6 kN at 3 mm deflection and achieving $120 \text{ kN}\cdot\text{mm}$ total toughness. The 2.0% curve marginally underperforms the 1.5% case (peak 10.2 kN, toughness $110 \text{ kN}\cdot\text{mm}$), confirming that beyond 1.5% the benefits of additional fibres are outweighed by the compaction and dispersion penalties introduced by fibre balling. The progressive transition from brittle to ductile failure mode with increasing fibre content is the central finding illustrated by Figure 4. This behaviour is mechanically explained by the crack-bridging mechanism: as the matrix cracks, individual fibres spanning the crack faces resist opening through a combination of interfacial bond and mechanical interlock provided by the embossed surface texture. Each fibre that progressively debonds and pulls out dissipates energy, sustaining load well beyond first crack. At 1.5%, the fibre network is dense enough to engage multiple fibres across any given crack plane, producing the observed distributed softening response rather than a single catastrophic fracture.

Figure 1 — Load-Deflection Curves: 60 mm Fibres, All Volume Fractions (Two-Point Loading per IS 516, $100\times 100\times 500 \text{ mm}$ Prisms)

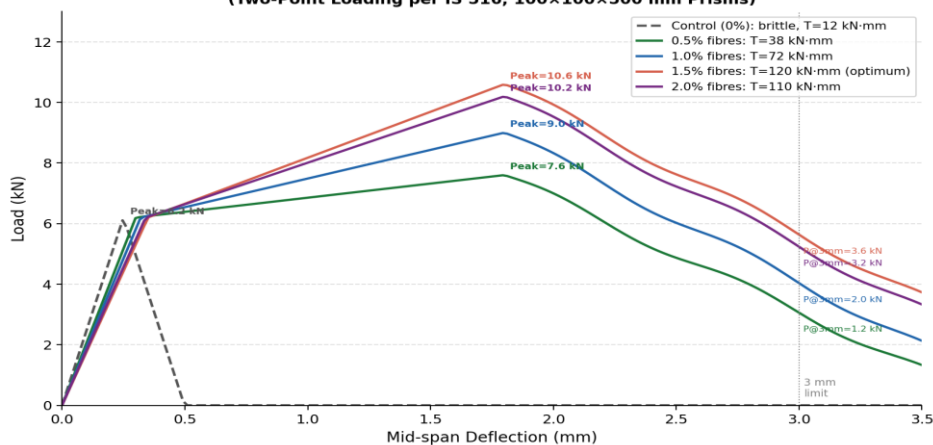


Figure 4 — Load-Deflection Curves: 60 mm Fibres, All Volume Fractions (IS 516, $100\times 100\times 500 \text{ mm}$ Prisms)

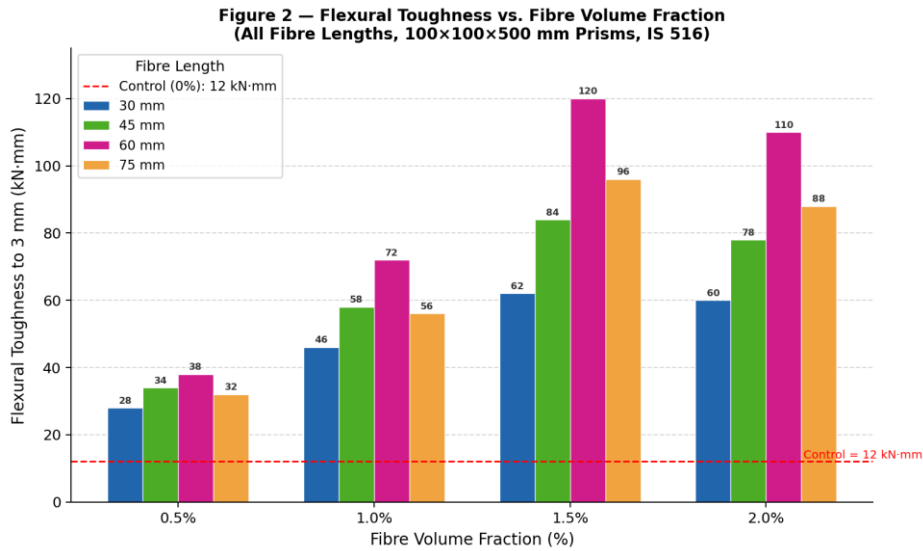


Figure 2 — Flexural Toughness to 3 mm vs. Fibre Volume Fraction (All Fibre Lengths, IS 516)

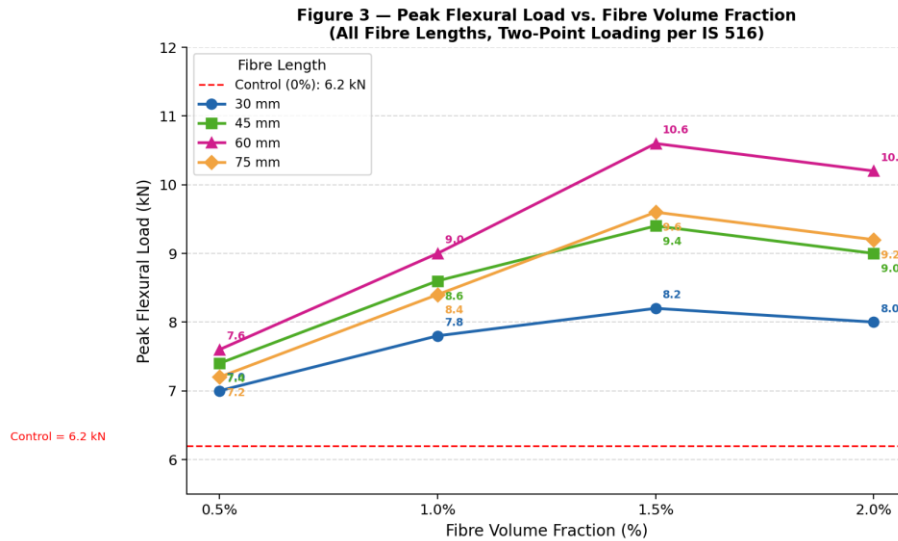


Figure 3 — Peak Flexural Load vs. Fibre Volume Fraction (All Fibre Lengths, IS 516)

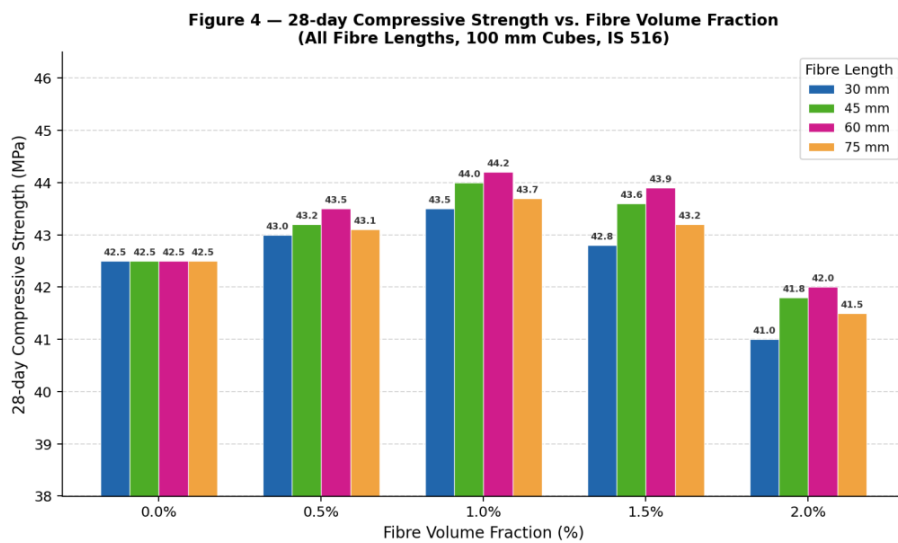


Figure 1 — 28-day Compressive Strength vs. Fibre Volume Fraction (All Fibre Lengths, IS 516)

8. DISCUSSION

Optimum Fibre Content: Results indicate 1.5% by volume is the optimum fibre content. At this dosage the flexural toughness is maximised and residual strength is highest, while compressive strength is retained within ±5% of the control. These findings are consistent with literature on plastic fibre-reinforced concrete, where optimum dosages in the range 0.5–1.5% by volume are widely reported [16, 20, 21].

Effect of Fibre Length: Among the four fibre lengths studied, 60 mm fibres provide the best overall performance. Fibres of this length are long enough to effectively bridge macro-cracks and develop adequate fibre–matrix bond over their embedment length, yet short enough to avoid severe balling and mixing difficulties. The 75 mm fibres achieve comparable toughness at 1.5% but present greater practical challenges during mixing, consistent with findings by Kevern [26] on the interplay between fibre length and workability.

Effect on Compressive Strength: Short fibres (30 mm, 45 mm) show marginal improvements at 1.0% due to micro-crack arrest [25]. Longer fibres (60 mm, 75 mm) yield slightly higher compressive strength improvements owing to improved matrix confinement. At 2.0% fibre volume, all lengths show a reduction in compressive strength (1–4 MPa below control), consistent with increased entrapped air and incomplete compaction, as reported by Sarker [14, 28] and Thomas [29].

Workability Trade-off: Workability, measured as slump, decreases monotonically with increasing fibre content. Beyond 1.5%, fibre balling and significant slump reduction reduce practical applicability. Superplasticizer dosage must be adjusted progressively per IS 9103 [11] to maintain adequate workability. A slump of approximately 55 mm at 1.5% fibre content remains within the range suitable for conventional vibrated placement (IS 456 [10] workability class: medium).

Activator System and Geopolymer Chemistry: The alkaline activator system employing 12 M NaOH and $\text{Na}_2\text{SiO}_3/\text{NaOH} = 2.5$ is consistent with the established optimum reported by Hardjito and Rangan [13]. The alkaline activation mechanism of fly ash is well established [22]. The corrected activator-to-binder ratio of 0.40 is within the published optimum range of 0.40–0.50 for fly ash–OPC hybrid geopolymers [32]. Compressive strength in fly ash geopolymers is influenced by activator concentration, curing temperature, and Si/Al ratio [24]. The hybrid inclusion of 30% OPC facilitates ambient-temperature setting and enhances early strength development by providing calcium silicate hydrate (C–S–H) alongside the N–A–S–H geopolymer gel [34].

Comparison with Literature: Results align qualitatively with Indian and international studies on plastic fibres in OPC and geopolymer concrete [16, 27, 28]. Geopolymer concrete for structural applications has been shown to achieve competitive mechanical properties [23]. The ductility transformation observed in this study is consistent with findings on engineered cementitious composites [19] and high-performance fibre-reinforced concretes [17], and with general fibre reinforced concrete design principles [30, 31]. Geopolymer–OPC hybrid matrices may exhibit somewhat different fibre–matrix bond characteristics compared with pure OPC matrices, owing to the different nature of the C–S–H / N–A–S–H interfacial transition zone. Microstructural confirmation via scanning electron microscopy is recommended.

Limitations: Microstructural interactions (fibre pull-out vs. rupture, interfacial transition zone) should be confirmed by scanning electron microscopy and pull-out tests. Curing regime sensitivity requires careful temperature and duration control. Long-term durability (shrinkage, creep, chloride resistance) was not evaluated in the present study.

9. CONCLUSIONS

- A dosage of 1.5% by volume of embossed straight polypropylene fibres (0.6 mm diameter) yields the best overall flexural performance in the hybrid geopolymer concrete studied, particularly when combined with 60 mm fibre length.
- Compressive strength is largely retained up to 1.5% fibre volume and declines at 2.0% owing to compaction difficulties and entrapped air. The maximum strength variation relative to control is within $\pm 5\%$.
- Flexural toughness (energy absorption to 3 mm deflection) increased by up to 10 times compared to the control for the best combination (60 mm fibres, 1.5% volume fraction). Peak flexural load increased by approximately 70% for the same combination.
- The alkaline activator system (12 M NaOH; $\text{Na}_2\text{SiO}_3/\text{NaOH} = 2.5$; activator-to-binder ratio = 0.40; total binder = 420 kg/m³) is confirmed as appropriate for the target compressive strength of 40–45 MPa with oven curing at 60 °C for 24 hours.
- Practical implementation requires a carefully controlled mixing sequence, pre-prepared alkaline activator solution, and progressive superplasticizer adjustment to avoid fibre balling at dosages of 1.0% and above.
- Future work should include scanning electron microscopy to characterise the fibre–matrix interfacial transition zone and pull-out tests to distinguish fibre rupture from pull-out failure modes.

ACKNOWLEDGMENT

The authors acknowledge the support of the Department of Civil Engineering, Jain Deemed to be University, for providing laboratory facilities and resources for this research work.

10. REFERENCES

- [1] IS 12269:2013 — Specification for 53 Grade Ordinary Portland Cement. Bureau of Indian Standards, New Delhi.
- [2] IS 3812 (Part 1):2003 — Pulverized Fuel Ash for use as Pozzolana. Bureau of Indian Standards, New Delhi.
- [3] IS 383:2016 — Specification for Coarse and Fine Aggregates for Concrete. Bureau of Indian Standards, New Delhi.
- [4] IS 2386 (Parts 1–8) — Methods of Test for Aggregates for Concrete. Bureau of Indian Standards, New Delhi.
- [5] IS 10262:2019 — Concrete Mix Proportioning — Guidelines. Bureau of Indian Standards, New Delhi.
- [6] IS 1199 (Part 1):2018 — Sampling of Fresh Concrete. Bureau of Indian Standards, New Delhi.
- [7] IS 1199 (Part 2):2018 — Determination of Consistency of Fresh Concrete (Slump Test). Bureau of Indian Standards, New Delhi.
- [8] IS 516 (Part 1, Sec 1):2018 — Hardened Concrete — Compressive Strength. Bureau of Indian Standards, New Delhi.
- [9] IS 516 (Part 5, Sec 1):2018 — Hardened Concrete — Flexural Strength (Beams). Bureau of Indian Standards, New Delhi.
- [10] IS 456:2000 — Code of Practice for Plain and Reinforced Concrete. Bureau of Indian Standards, New Delhi.
- [11] IS 9103:1999 — Specification for Admixtures for Concrete. Bureau of Indian Standards, New Delhi.
- [12] Davidovits, J., *Geopolymer Chemistry and Applications*, 4th ed., Institut Géopolymère, Saint-Quentin, 2015.
- [13] Hardjito, D. and Rangan, B. V., "Development and Properties of Low-Calcium Fly Ash-Based Geopolymer Concrete," Research Report GC 1, Curtin University of Technology, Perth, 2005.
- [14] Sarker, P. K., "Geopolymer concrete: A review of development and research," *Construction and Building Materials*, vol. 93, pp. 1264–1271, 2015.
- [15] Bentur, A. and Mindess, S., *Fibre Reinforced Cementitious Composites*. Elsevier Applied Science, London, 1990.
- [16] Banthia, N. and Gupta, R., "Influence of polypropylene fibre geometry on plastic shrinkage cracking in concrete," *Cement and Concrete Research*, vol. 36, no. 7, pp. 1263–1267, 2006.
- [17] Yoo, D.-Y. and Banthia, N., "Mechanical and structural behaviours of ultra-high-performance fiber-reinforced concrete subjected to impact and blast," *Construction and Building Materials*, vol. 149, pp. 416–431, 2016.
- [18] ASTM C1609/C1609M, *Standard Test Method for Flexural Performance of Fiber-Reinforced Concrete*. ASTM International, West Conshohocken, PA.
- [19] Li, V. C., "On engineered cementitious composites (ECC): A review of the material and its applications," *J. Advanced Concrete Technology*, vol. 1, no. 3, pp. 215–230, 2003.
- [20] Nataraja, M. C., "Performance of polypropylene fibre reinforced concrete," *Indian Concrete Journal*, vol. 75, no. 9, pp. 571–575, 2001.
- [21] Nematollahi, B. and Sanjayan, J., "Effect of different superplasticizers and activator combinations on workability and strength of fly ash-based geopolymer," *Materials and Design*, vol. 57, pp. 667–672, 2015.
- [22] Palomo, A., Grutzeck, M. W. and Blanco, M. T., "Alkali-activated fly ashes: A cement for the future," *Cement and Concrete Research*, vol. 29, no. 8, pp. 1323–1329, 1999.
- [23] Rangan, B. V., "Geopolymer concrete for structural applications," *Indian Concrete Journal*, vol. 88, no. 5, pp. 42–48, 2014.
- [24] Soutsos, M. N., et al., "Factors influencing the compressive strength of fly ash based geopolymers," *Construction and Building Materials*, vol. 110, pp. 355–368, 2016.
- [25] Mehta, P. K. and Monteiro, P. J. M., *Concrete: Microstructure, Properties, and Materials*, 4th ed. McGraw-Hill, New York, 2014.
- [26] Kevern, J. T., "Evaluation of pervious concrete workability using the rod drop test," *J. Testing and Evaluation*, vol. 37, no. 6, 2009.
- [27] Li, M., "Bond behavior of polymeric fibres in cementitious matrices," *J. Materials Science*, vol. 47, no. 8, pp. 3629–3637, 2012.
- [28] Sarker, P. K., "Polypropylene fibre reinforced geopolymer concrete: An experimental investigation," *Materials and Structures*, vol. 50, no. 1, 2017.
- [29] Thomas, M. S., "Effect of fibre content on workability and strength of concrete," *Construction Materials Journal*, vol. 163, no. CM4, pp. 209–215, 2010.
- [30] Nawy, E. G., *Concrete Construction Engineering Handbook*, 2nd ed. CRC Press, Boca Raton, 2008.
- [31] Banthia, N., "Fibre reinforced concrete: Design and applications," *Indian Concrete Journal*, vol. 86, no. 5, pp. 9–22, 2012.
- [32] Patankar, S. V., Jamkar, S. S. and Ghugal, Y. M., "Effect of water-to-geopolymer binder ratio on the production of fly ash based geopolymer concrete," *Int. J. Advanced Technology in Civil Engineering*, vol. 2, no. 1, pp. 79–83, 2013.
- [33] Ferdous, M. W., Kayali, O. and Khennane, A., "A detailed procedure of mix design for fly ash based geopolymer concrete," 4th Asia-Pacific Conference on FRP in Structures, Australia, December 2013.
- [34] Fernández-Jiménez, A. and Palomo, A., "Composition and microstructure of alkali activated fly ash binder: Effect of the activator," *Cement and Concrete Research*, vol. 35, no. 10, pp. 1984–1992, 2005.
- [35] Habert, G., d'Espinose de Lacaillerie, J. B. and Roussel, N., "An environmental evaluation of geopolymer based concrete production: reviewing current research trends," *Journal of Cleaner Production*, vol. 19, no. 11, pp. 1229–1238, 2011.
- [36] MoEFCC (Ministry of Environment, Forest and Climate Change), "Fly Ash Utilization: Status and Initiatives," Government of India Report, New Delhi, 2022.
- [37] Sivakumar, A. and Santhanam, M., "Mechanical properties of high strength concrete reinforced with metallic and non-metallic fibres," *Cement and Concrete Composites*, vol. 29, no. 8, pp. 603–608, 2007. (Aspect ratio effects on fibre-reinforced composites.)